Bioelectrochemistry 121 (2018) 169–175

Contents lists available at ScienceDirect

Bioelectrochemistry

journal homepage: www.elsevier.com/locate/bioelechem

Characterization and electrochemical response of DNA functionalized 2 nm gold nanoparticles confined in a nanochannel array

Ana S. Peinetti [a], Helena Ceretti [b], Martín Mizrahi [c], Graciela A. González [a], Silvana A. Ramírez [b], Félix G. Requejo [c], Javier M. Montserrat [b], Fernando Battaglini [a,*]

[a] INQUIMAE (CONICET), Departamento de Química Inorgánica, Analítica y Química Física, Facultad de Ciencias Exactas y Naturales, Universidad de Buenos Aires, Ciudad Universitaria, Pabellón 2, C1428EHA Buenos Aires, Argentina
[b] Universidad Nacional de Gral. Sarmiento, J. M. Gutierrez 1150, B1613GSX Los Polvorines, Prov. de Bs. As., Argentina
[c] Instituto de Investigaciones Físicoquímicas Teóricas y Aplicadas – INIFTA, CONICET y Dto. Química, Fac. Cs Ex, UNLP, 1900 La Plata, Argentina

ARTICLE INFO

Article history:
Received 20 November 2017
Received in revised form 2 February 2018
Accepted 7 February 2018
Available online 09 February 2018

ABSTRACT

Polyvalent gold nanoparticle oligonucleotide conjugates are subject of intense research. Even though 2 nm diameter AuNPs have been previously modified with DNA, little is known about their structure and electrochemical behavior. In this work, we examine the influence of different surface modification strategies on the interplay between the meso-organization and the molecular recognition properties of a 27-mer DNA strand. This DNA strand is functionalized with different sulfur-containing moieties and immobilized on 2 nm gold nanoparticles confined on a nanoporous alumina, working the whole system as an electrode array. Surface coverages were determined by EXAFS and the performance as recognition elements for impedance-based sensors is evaluated. Our results prove that low DNA coverages on the confined nanoparticles prompt to a more sensitive response, showing the relevance in avoiding the DNA strand overcrowding. The system was able to determine a concentration as low as 100 pM of the complementary strand, thus introducing the foundations for the construction of label-free genosensors at the nanometer scale.

1. Introduction

Gold represents one of the most useful surfaces as transduction element in sensor construction. Its ability to undergo fast electron transfer and optical properties open a myriad of options for surface modification and transduction techniques (e.g. QCM, SPR, electrochemistry), enhanced by its ability to be easily modified by thiol derivatives [1].

On the other hand, DNA single stranded oligonucleotides are booming as one of the most adaptable recognition elements. First, it was used as genosensors in the diagnosis of congenital diseases [2–6], later on as molecular recognition elements (aptamers) [7] and as artificial enzymes (DNAzymes) [8,9]. Oligonucleotide DNA synthesis allows the incorporation of chemical modifications at defined positions. This feature is very important because of the introduction of moieties capable to act as anchors on the surface of the sensors. Well known examples are the modifications carried out with the avidin/biotin system [10,11] and thiol groups [12–14]. Finally, oligonucleotide strands undergo conformational changes during the recognition process that can be exploited to gain sensitivity in the signal generation [10,11,15].

In DNA based sensors, the immobilized strand on the gold surface has to maintain its recognition ability; this is accomplished by controlling the strand orientation and spatial distribution. Therefore, the DNA gold nanoparticle interface is a key point for the design of functional hybrid nanoplatforms. One way to achieve this goal is the co-immobilization of other thiol-compound along with the thiol modified DNA [13,16]. An alternative to thiol-modified strands is the replacement of one of the non-bridging oxygen atom of the phosphate group in the DNA strand by sulfur, generating a phosphorothioate moiety (PS). This immobilization strategy was recently employed on gold nanoparticles [17] and gold electrodes [16]. The use of PS is appealing not only because of the sulfur-based anchoring but also due to the advantages regarding costs and synthetic procedures [16,17].

Modification of gold nanoparticles with sulfur terminated DNA probes represents a useful technique. Most of the results presented in the literature correspond to suspended nanoparticles over 10 nm diameter; while the conjugation of 2 nm diameter gold nanoparticles has been scarcely studied. Mirkin's group was able to characterize 2-nm gold nanoparticle-oligonucleotide conjugates [18]; however, no further reports have been presented, even though the final properties of the functionalized nanomaterials depend on the geometry and the environment of the nano-biointerface [19]. Recently, we have introduced the synthesis of AuNPs below to 2 nm diameter as a nanoelectrode array

* Corresponding author.
E-mail address: battagli@qi.fcen.uba.ar (F. Battaglini).

https://doi.org/10.1016/j.bioelechem.2018.02.002
1567-5394/

confined in an alumina matrix showing a good electrochemical response and the ability to work as a sensor for different analytes [15,20].

In this work, we present a systematic study on different strategies regarding the conjugation of DNA terminated with different sulfur derivatives on 2 nm diameter AuNP confined in nanoporous alumina and the impact on the sensitivity as an impedimetric sensor. Three different immobilization strategies based on S-surface modification were tested, involving three types of terminal sequences: thiol, disulfide bridge and phosphorothioate thymidine. Our results demonstrated that the immobilization procedure has a relevant role in the amount of DNA immobilized and, consequently, in the sensitivity of the recognition process. Also, we compare the effect of a negatively charged redox probe with a neutral probe in an electrochemical impedance spectroscopy (EIS) assay to determine if the volume exclusion effect prevails over the charge repulsion in this confined system. As a proof of concept, a 27-mer DNA strand was quantified in a concentration as low as 100 pM.

2. Experimental

2.1. Reagents

All reagents were analytical grade. Water (18 MΩ cm) was provided by a Millipore Simplicity equipment. Oligonucleotide sequences, desalted and HPLC purified, were used as provided (Sigma-Genosys). 27-mer DNA strand sequence was the original Szostak's AMP-binding aptamer sequence [21] plus five additional thymidines as linker.

Disulfide sequence (RS − SDNA):

5′-[C_6H_{13}-S-S-C_6H_{12}]TTTTTACCTGGGGGAGTATTGCGGAGGAAGGT-3′

Phosphorothioate sequence (5PSDNA, Ts: thymidine phosphorothioate):

5′-TsTsTsTsTsTTTTTACCTGGGGGAGTATTGCGGAGGAAGGT-3′

Complementary strand

5′-ACCTTCCTCCGCAATACTCCCCCAGGT-3′

Random complementary strand

5′-CTATCCAATCCCCTTGACTCGGCCCCA-3′

2.2. Nanoporous alumina and gold nanoparticles synthesis

Working electrodes (4 mm^2) were prepared as follow: Aluminum 1145 (99.5%) was degreased with acetone in an ultrasonic bath, followed by electropolishing in a 5:1 ethanol:$HClO_4$ solution (v:v) at 18 V for 1 min. The clean surface was immediately exposed to 15% H_2SO_4 at room temperature (15 V, 1 min), using a lead plate as counter electrode. Once the electrode was anodized, it was left 5 min in the acid electrolyte and then rinsed with MilliQ water. Pore size and depth were characterized by scanning electron microscopy [15].

Gold electrodeposition was carried out using an electroplating commercial solution containing $K[Au(CN)_2]$ (15 g L^{-1}). Anodized aluminum and a gold plate were used as working and counter electrodes, respectively. Gold electrodeposition was performed in three steps: i) metal deposition at −3 mA cm^{-2} for 8 ms; ii) 3 mA cm^{-2} (2 ms) to decrease the capacitive oxide layer and interrupt the electric field at the interface where it is being deposited; iii) 0 mA cm^{-2} (500 ms) to recover the ion concentration in the pores by diffusion from the solution. Steps i) to iii) were repeated 3000 times.

2.3. Gold surface modification

AuNP synthesized inside the nanoporous alumina were modified by immobilization of the sulfur-modified strands previously described. The electrodes were incubated with 10 μL of the corresponding DNA sequence solution (1 μM final concentration) for 30 min at room temperature, and rinsed with buffer prior to use. Three different strategies of S-Au quimisorption were employed [22]: i) RS + SDNA method, where the thiol-terminated sequence is prepared by homogeneous reduction with tris(2-carboxyethyl)phosphine (TCEP) (1.5 mM) for 2 h at room temperature in the dark [21]. In this way, an equimolar mixture of hexanethiol and thiol-terminated DNA is obtained (RS + SDNA) and is exposed to the working electrode. ii) RS − SDNA method, where the DNA sequence ending in a disulfide bridge is directly adsorbed on the gold surface. iii) 5PSDNA method, the same DNA sequence containing a 5 phosphorothioate thymidine tag is directly adsorbed on the gold surface.

2.4. X-ray techniques

Nanoparticle size and sulfur coverage in the nanoparticles were determined by Extended X-Ray Absorption Fine Structure (EXAFS). Au L3-edge EXAFS spectra were measured at room temperature in fluorescence mode at the XAFS2 beam line at the Laboratorio Nacional de Luz Sincrotron (LNLS, Campinas, Brazil). An ionization chamber was used to detect the incident flux and a 15-element germanium solid state detector was used to sense the fluorescence signal from the sample. Data were processed using ATHENA with the AUTOBK background removal algorithm [23].

The energy of the incident photons was calibrated using a metallic gold film. The EXAFS oscillations $\chi(k)$ were extracted from the experimental data with standard procedures using the Athena program. The k^2 weighted $\chi(k)$ data, to enhance the oscillations at higher k, were Fourier transformed. The Fourier transform was calculated using a Hanning filtering function. EXAFS modeling was carried out using the ARTEMIS program which is part of the IFFEFIT package [23].

2.5. Quartz crystal balance measurements (QCM-D)

QCM-D experiments were performed using a Q-Sense instrument (QCM-D, Q-Sense E1, Sweden) equipped with a Q-Sense Flow Module (QFM 401). For all measurements QSX 301 gold sensors were used. Samples were perfused using a peristaltic microflow system (ISMATEC, ISM 596D Glattbrugg, Switzerland). Measurements were recorded at several odd multiples of the fundamental frequency (overtones) and frequency shifts were normalized dividing by the overtone number. Data corresponding to the 3rd overtone were employed for calculations in Table 2.

2.6. Electrochemical measurements

Hybridization experiments were carried out by exposing the DNA modified electrodes to Tris buffer (50 mM, pH 7.4) containing the complementary strand (0.1–500 nM) during 30 min at room temperature. Each determination was carried out in a new electrode by triplicate. A solution containing 50 mM $K_4[Fe(CN)_6]$ in HEPES buffer (50 mM, pH 7.4) was employed as redox probe. In AMP recognition experiments, electrodes were incubated during 30 min at room temperature with 500 nM AMP solution prepared in Tris buffer (50 mM, pH 7.4). A similar protocol was used for complementary strands.

EIS was performed at the formal potential of the redox probe, 0.20 V vs Ag/AgCl using a frequency range from 10 kHz to 1 Hz. Voltage amplitude was 10 mV. Determinations were performed by immersing the electrode in the probe solution before and after incubation with the complementary strand or AMP. Data were represented as Nyquist plots. The electrical parameters were obtained by fitting the impedance spectroscopy data from 10 to 10,000 Hz for each experiment to an equivalent circuit that included the following elements: the electrolyte resistance (Rs) in series with two branches in parallel, one corresponding to the electron transfer resistance (Ret) and the other to a constant phase element (CPE), representing the non-ideal behavior of the double layer as a capacitor. Fitting was carried out using EchemAnalyst™ Software. The difference between Ret after and prior hybridization or AMP incubation (ΔRet) was used as signal.

3. Results and discussion

3.1. AuNP-DNA conjugate characterization

Different strategies are available for preparing AuNP-DNA conjugates, several of them are based on the Au—S bond, including direct adsorption of alkylthiol, multisulfide or phosphorothioate terminated oligonucleotides [15,17,24]. Tandem phosphorothioate modification of gold has been recently used as an alternative to thiol groups due to its lower cost in studies involving DNA mediated electron transfer [16], aptasensor construction [12] or nanoparticle modification [17]. On the other hand, alkylthiol derivatives are known for its great versatility [15,17]. However, the efficiency of these immobilization processes and their sensitivity as biorecognition elements in confined nanostructures were not previously studied.

The AuNP modification was tested by using three different strategies (Schematic 1), expecting that the confinement of this small AuNPs has a positive impact on the surface modification and in the response of the final nanodevice. The first method consists in the immobilization of DNA with an equimolar mixture of hexanethiol and thiol-tagged DNA (RS + SDNA, Schematic 1, top). The second immobilization process uses a disulfide moiety, where one sulfur is bound to the DNA and the other to an aliphatic six carbon chain, directly exposed to the AuNPs, where the S—S bond is broken due to its reduction and both the DNA and the hexane S-terminated chain bind to the surface (RS — SDNA, Schematic 1, middle). In this way, it can be assumed that the relationship between DNA and hexanothiol that binds to the AuNP surface is 1:1. The third option comprises a terminal modification containing 5 phosphorothioate derivatized thymines where one of the non-bridging oxygens is replaced by sulfur (5PSDNA, Schematic 1, bottom).

The extent of the modification of the 2 nm AuNPs inside the porous alumina matrix was determined by extended X-ray absorption fine structure (EXAFS). This technique provides information about the local environment of Au atoms, i.e. the number, type and distances between neighboring Au atoms without altering the sample allowing to establish the size and modification of the generated AuNPs (Fig. 1 and Table 1).

The RS + SDNA modification method yields a nanoparticle sulfur coverage of ca. 60%. The Au-S coordination shell is indicated in the Fourier transform of the EXAFS oscillation (Fig. 1, blue dotted line). This represents a high sulfur coverage, which suggests that most of the surface exposed to the solution has been modified. The ratio between alkanethiol molecules and gold atoms for 2 nm diameter AuNPs was previously determined by Au-L3 EXAFS, yielding a 2:3 value [25]. This result indicates that practically the maximum coverage is obtained and can be mainly related to the hexanethiol since the alkyl derivatives can be densely packed due to its structure.

When the RS — SDNA method was tested, the sulfur coverage observed was 35%. In this case, as one DNA strand was adsorbed along with one hexanethiol, the repulsion between the charged strands plays an important role, decreasing the coverage of the AuNP. Finally, the phosphorothioate DNA produced a sulfur coverage slightly above to the observed for the RS — SDNA method (41% vs 35%). However, it must be considered that two S atoms are introduced per DNA sequence in the case of RS — SDNA method while five S atoms are introduced per DNA sequence in the case of 5PSDNA method. This difference in the binding moiety led to a final coverage of around 17% when the RS — SDNA method is used, and around 8% for the phosphorothioate. Considering that 2/3 of the nanoparticle surface is exposed to the solution and estimating the number of gold atoms in the surface from its diameter [26], the active AuNP consists of ca. 65 atoms. This means that 7 and 3 strands are immobilized on each NP for the RS-DNA and 5PSDNA modifications, respectively. These nanoparticle modifications are similar to the previously reported by Mirkin's group for this AuNP size [18] where a value of 5 strands was obtained for a strand of similar length. For the RS + SDNA method, the amount of DNA adsorbed is uncertain and probably lower due to the competition with hexanethiol. The degree of conjugation will have an important effect on the electrochemical response.

On the other hand, it is possible to determine the moles of DNA adsorbed on a planar surface for each modification procedure using a quartz crystal balance. Table 2 shows the obtained values, and percentages respect to the possible maximum for a planar surface

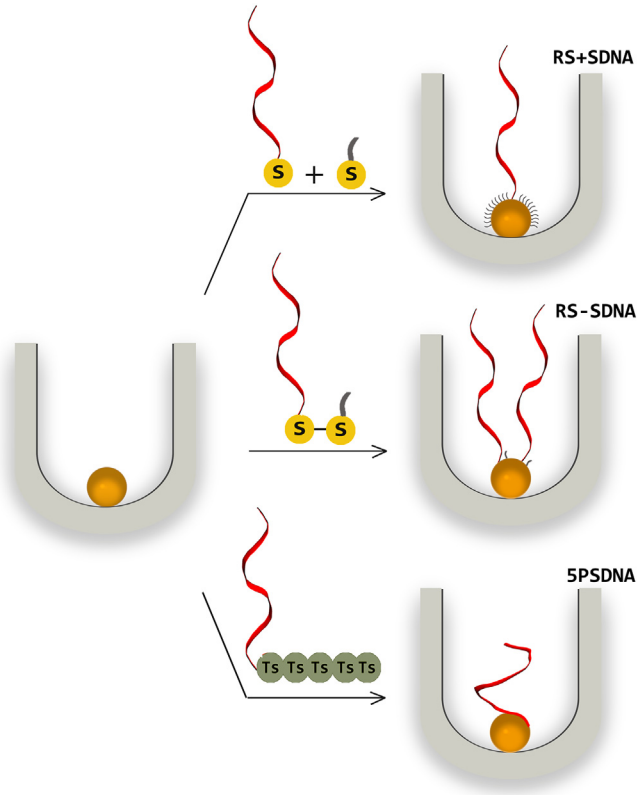

Schematic 1. AuNP modification procedures used in this work. Top: coadsorption (RS + SDNA); middle: disulfide sequence (RS — SDNA); bottom: 5 phosphorothioate thymidine tagged sequence (5PSDNA).

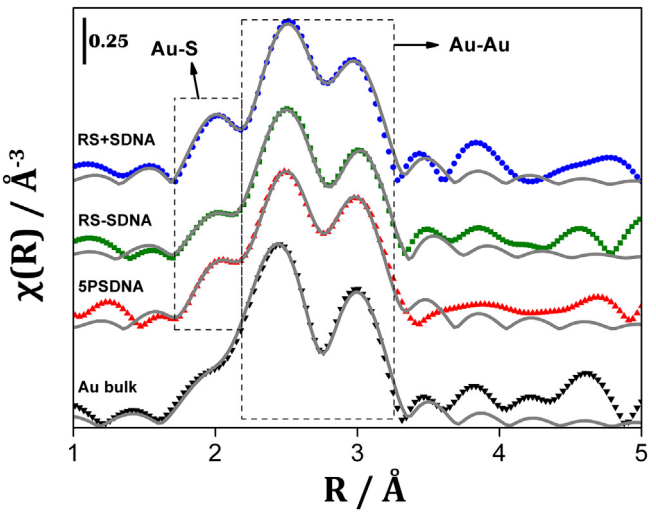

Fig. 1. Fourier transform of the Au-L3 EXAFS oscillation (without phase correction) for AuNP modified with: RS + SDNA (blue circles), RS — SDNA (green squares), 5PSDNA (red upward triangles) and bulk gold (black downward triangles). The fitting curves are represented in grey lines. (For interpretation of the references to color in this figure legend, the reader is referred to the web version of this article.)

Table 1
Fitted values from EXAFS signal.

Sample	L_3-Au							
	N_{Au-Au}	R_{Au-Au}(Å)	$\sigma\sigma^2_{Au-Au}$(Å)	N_{Au-S}	R_{Au-S}(Å)	σ^2_{Au-S}(Å^2)	Sup S:Au	Au Np size (nm)
Au bulk	12	2.880(2)	0.0082(3)	–	–	–	–	–
AuNP/RS + SDNA	9.8(8)	2.836(5)	0.0075(6)	0.22(8)	2.340(5)	0.003(1)	0.60	2.3(7)
AuNP/RS − SDNA	9.7(9)	2.847(6)	0.0075(6)	0.13(7)	2.330(5)	0.003(1)	0.35	2.3(7)
AuNP/5PSDNA	9.6(8)	2.840(4)	0.0076(6)	0.15(8)	2.337(6)	0.003(1)	0.41	2.2(7)

Average coordination number (N), interatomic distance (R) and Debye-Waller factor (σ^2), for the first coordination shell around Au atoms, together with the estimated superficial S:Au atomic ratio and diameter for the samples. The coordination number was fixed at 12 for metallic Au.

(780 pmol cm^{-2}) [27]. It is interesting to confront the amount of adsorbed strands for the RS + SDNA and RS − SDNA methods, which is lower when the strand competes with the hexanethiol for the gold atoms. Comparing this results with the degree of modification for the 2 nm AuNP, it can be observed that the modification of the AuNP is 3 times greater than the one obtained for the planar surface.

3.2. Molecular recognition and electrochemical response

Electrochemical impedance spectroscopy (EIS) is an effective method for probing binding events between a recognition element immobilized on a conductive surface and the target molecule. The formation of such complexes commonly alters the capacitance and the resistance at the surface electrolyte interface. This is mainly due to charge changes in the surface, reflected in changes in capacitance, and hindrance effects as the target molecule binds to the surface, reflected in changes in the resistance. The application of this principle to the development of label-free sensors has been extensively discussed [28].

The 27-mer single strand DNA used to modify the AuNP shows two interesting features. This 27 oligonucleotide strand has a size close to those of micro-RNA that have taken great impulse as biomarkers for several diseases in the last years [29] and, on the other hand, the sequence corresponds to an AMP-binding aptamer [21]. In this way, two different applications of the same strand can be compared (Schematic 2); as an aptamer, where a stem-loop configuration is obtained when AMP is recognized with a dissociation constant of 6×10^{-6} [30], and as a complementary strand, where a double helix is formed with a complementary sequence and a dissociation constant estimated in 6×10^{-21} [31,32]. Issues regarding conformational change, binding affinity, hindrance and charge effects can be addressed using this probe.

Fig. 2 shows the impedance spectra of the three types of modified AuNP electrode arrays exposed to a ferrocyanide solution. Black square traces correspond to the response of the naked nanoparticles, while the triangles correspond to the modified surfaces.

Even though EIS has been extensively used as an analytical tool for label-free molecular recognition assays, most of the work is related to the study of the electron transfer process on a planar electrode coupled with a semi-infinite linear diffusion process. This system can be described through an equivalent circuit that combines a resistance (the electron transfer process), a capacitor (due to the double layer formed at the interface electrode/solution) and a Warburg diffusion impedance [28,33].

In our case, as an array of recessed nanoelectrodes is used, the diffusional field formed depends on three factors: time scale, electrode radius and interelectrode distance, which in turn produce four different diffusional patterns illustrated in Schematic 3 [34]. Case 1 corresponds to a diffusional field at high frequency (shortest time) and can be described by planar diffusion; therefore, it can be treated using a Warburg impedance element. Case 2 can be treated as individual nanoelectrodes, generating a semi-spherical diffusional field around each one, which in turn produces a flattened semi-circle in the Nyquist plot when the process is controlled by the probe diffusion [35,36]. Case 3 is more complex since the overlapping of the adjacent diffusional layers forbids its treatment as independent nanoelectrodes. However, the diffusional fields are not so heavily overlapped as in Case 4, which is equivalent to a linear diffusion case corresponding to the lowest frequencies, i.e. longest time.

The naked gold nanoelectrodes present a complex behavior sweeping the different cases as the frequency changes, therefore it is difficult to apply a simple model. Instead, once the array is modified with the single DNA strand, an important change in the electron transfer process is observed, and a kinetic control of the process is observed for frequencies above 10 Hz. In these conditions, a simple model (Fig. 2, right, see inset) can be used which comprises the solution resistance (Rs), the electron transfer process as a resistance (Ret) and a constant phase element (CPE), that models the complex capacitive behavior of the recessed porous electrodes evidenced by a flattened semi-circle (note that the Z″ scale interval is a half of the Z′ interval) [37,38]. In this way, Ret values of 16.2, 32.1 and 30.3 kΩ were obtained for RS + SDNA, RS − SDNA and 5PSDNA methods, respectively. The more dramatic increase in the last two methods agrees with results obtained by EXAFS, where the higher DNA coverages are observed. Instead for the case of RS + SDNA method, the alumina pore size restriction acts as a barrier favoring the ingress of the alkylthiol at expenses of a lower amount of the DNA strand, the result is a high sulfur coverage, evidenced by EXAFS analysis, mainly due to the short alkylthiols and few DNA strands per nanoparticles. This result is corroborated by the smaller increase in the Ret after modification. In all cases we can assume that the signal change is mainly due to the few immobilized strands, introducing important hindrance and charge effects clearly observed for the RS − SDNA and 5PSDNA methods.

Table 2
Degree of DNA modification for Au planar surface and a 2 nm AuNP.

Modification procedure	Modified planar Au/pmol cm^{-2}	Modified planar Au/%	Modified 2 nm AuNP/%
RS + SDNA	26	3.5	Not determined
RS − SDNA	39	5.0	17
5PSDNA	13	1.7	8

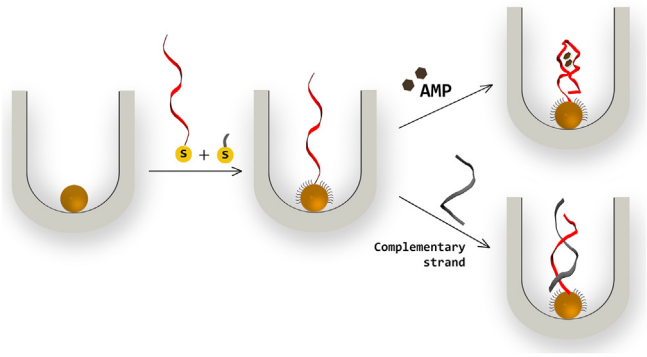

Schematic 2. Modification of AuNP by coadsorption of AMP-binding aptamer and hexanethiol followed by the application either to the recognition of AMP or the complementary strand.

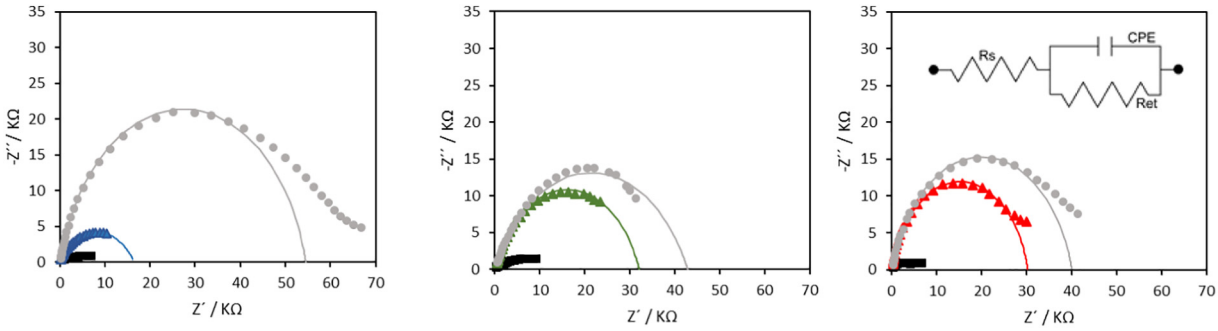

Fig. 2. EIS response to a 50 mM potassium ferrocyanide in 50 mM HEPES, pH 7.4. AuNPs (black squares); AuNPs/RS + SDNA (blue triangles, left panel), AuNPs/RS − SDNA (green triangles, center panel), AuNPs/5PSDNA (red triangles, right panel). EIS after incubation with 500 nM AMP are represented in grey circles. Inset in the right panel represents the equivalent circuit used to fit the data (continuous lines). EIS experimental data correspond to frequencies between 1 Hz to 10 kHz. Data was fitted between 10 Hz and 10 kHz. Details are given in the Experimental section. (For interpretation of the references to color in this figure legend, the reader is referred to the web version of this article.)

As the DNA strand used in this study is able either to bind AMP or its complementary part, we have chosen AMP to test how the different modifications affect the recognition process. The recognition event produces a conformational change from a random coil of 1 nm diameter to a rigid structure of 2 nm either by recognition of AMP (stem-loop) [39] or the complementary sequence (double helix) [40]; however, AMP is a small molecule that can easily diffuse through the alumina pores and it can be used at a relatively high concentration to ensure that the recognition process is evaluated. Therefore, the three electrode arrays were exposed to an AMP solution (Fig. 2). The impedance spectrum for the AuNP modified by the RS + SDNA method shows that the adsorbed DNA sequence can undergo an important conformational change when it is exposed to the target molecule ($\Delta Ret = 38.4\ k\Omega$); while in the other two cases the changes are smaller after AMP recognition, $\Delta Ret = 8.5$ and $9.7\ k\Omega$. These results lead to different hypothesis to explain this behavior in each case. The RS − SDNA method leads to the adsorption of more strands per nanoparticle, hindering the conformational changes required in the recognition process. On the other hand, the behavior observed in AuNP modified using the 5PSDNA method is in agreement with the experimental results already presented by Zhang et al. [41]. These authors analyzed this type of modification on AuNPs using SERS and SAXS techniques, concluding that the sulfur atom introduced on the phosphate backbone dominates the interaction between the DNA and the nanoparticle. The strand is most likely to be loaded in an approximate parallel orientation onto the particle surface, due to the multiple anchoring points. In this way, the surface is blocked with a highly negative charged oligonucleotide chain yielding a high electron transfer resistance, with no significant increase when the AMP recognition and the configuration change occurs. Finally, it can be concluded that the control of DNA surface coverage plays a key role in the sensitivity of the assay since the method introducing the lowest number of strands per nanoparticles (RS + SDNA) produces the more sensitive change.

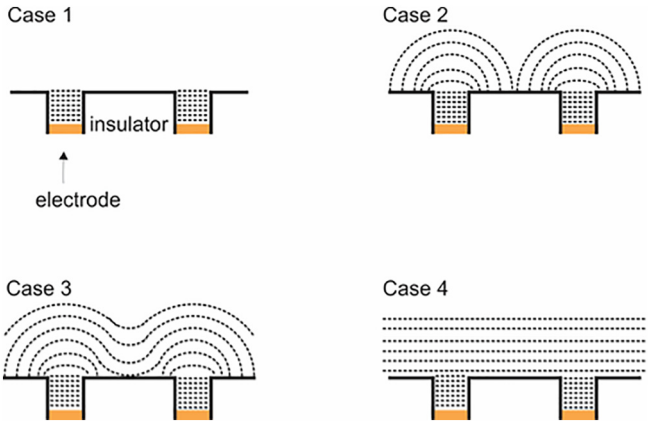

Schematic 3. Different cases for the diffusional field observed in recessed nanoelectrodes arrays. See text for details.

From the behavior observed, the modified surface should comply two conditions as an impedimetric sensor: 1) the strands should be separated from one another in such a way that no hindrance effects will reduce their ability to change their configuration in the recognition process, 2) after the recognition process, the change in the surface structure should produce a relevant modification in its electrical properties. These two conditions evolve in opposite directions, if the coverage density decreases, condition 1 can easily be fulfilled; however, the change in the surface electrical properties will be negligible, as in the case of planar gold electrode surface [15]. On the other hand, an excessive coverage, as in the case of 2 nm nanoparticles, will hamper the recognition process. Here, as the electrochemical response is the addition of the individual response of the NP confined in an insulating nanochannel, a low DNA coverage represents the best option to produce an important effect due to the configuration change when the recognition process is undertaken.

The repulsion between highly negative charged species like ferrocyanide and the oligonucleotide strands results in a very sensitive way to detect conformational changes on planar surfaces where the surface coverage of DNA represents a small fraction [33]. So far, we have exploited the structural change of the DNA sequence after the recognition process to explain the changes in the electron transfer resistance. However, it would be interesting to know if the charge repulsion prevails over the volume exclusion effect in this confined system. In order to consider this issue, ferrocenemethanol (a neutral probe) was tested. Fig. 3 shows that the modification of the surface with the DNA sequence and the further recognition event produced modifications in the EIS plot. The response was analyzed using the same equivalent circuit than before (Fig. 2, right, see inset) and taking into account the frequencies above 10 Hz, as result a change of the Ret from 71.6 kΩ to 91.8 kΩ can be estimated. The relative difference in electron transfer resistance due to the conformational change undergone in the recognition process is 28% when ferrocenemethanol is used. On the other hand, the same experiment carried out with ferrocyanide as a probe produces a change of 260% (Fig. 2, left). Therefore, the electrostatic interaction between the redox probe and the anchored oligonucleotide sequence remains as the main factor in the sensitivity of the assay.

Finally, we tested the ability of these confined and modified nanoparticles to recognize the complementary strand and to study how this recognition event affects the response of the modified nanoparticles that showed the greater sensitivity (RS + SDNA). Charge, affinity and configurational change may show some differences when compared to the binding of AMP. The binding of the complementary strand should introduce a greater increase in the whole charge of the nanoparticle, while the higher affinity will help to lower the detection limit. It is interesting to note that the size of the final structure should have a neutral

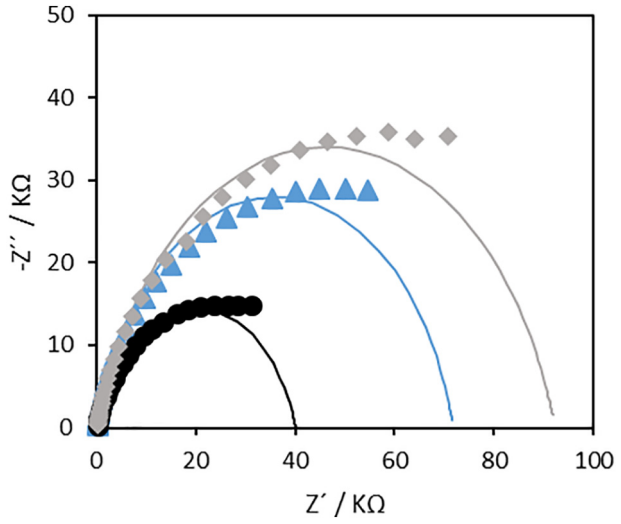

Fig. 3. EIS of 0.5 mM ferrocenemethanol in 50 mM HEPES, pH 7.4: AuNPs (black circles); AuNPs/RS + SDNA (blue triangles); AuNPs/RS + SDNA/AMP 500 nM (grey diamonds). EIS experimental data corresponds to frequencies between 1 Hz to 10 kHz. Data was fitted between 10 Hz and 10 kHz. (For interpretation of the references to color in this figure legend, the reader is referred to the web version of this article.)

effect since the formed double helix will have a 2 nm diameter, same diameter as the stem-loop formed by the AMP-DNA complex.

The RS + SDNA modified arrays were incubated with different concentrations of the complementary DNA strand. The change in electron transfer resistance is plotted against concentration (Fig. 4), showing that a complementary strand concentration as low as 100 pM can be easily detected. As a negative control, when this same array was exposed to a random strand (1 μM) the electron transfer resistance change was less than 1 kΩ, showing the selectivity of this system. It is interesting to note that a similar change in the electron transfer resistance (around 50 kΩ) is observed for 10 nM of the complementary strand and 500 nM of the AMP [15], suggesting that the charge and affinity of the complementary strand play an important role to improve the sensitivity of the assay.

The nanoparticle/nanoporous system shown here was able to work with 10 μL samples and to quantify a concentration of 10^{-10} M.

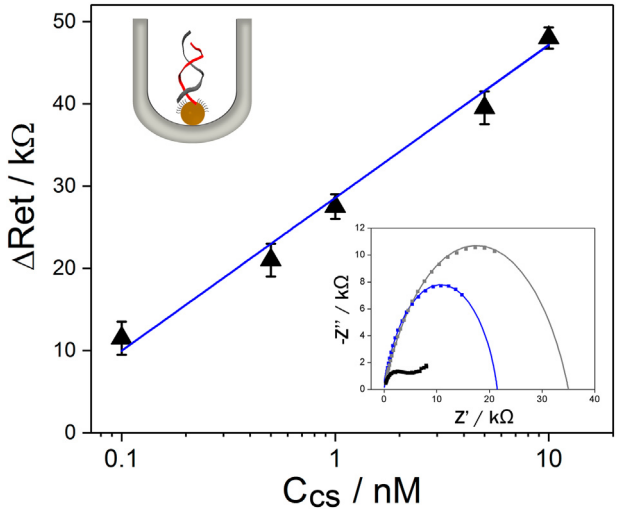

Fig. 4. Dependence of ΔRet with complementary strand (CS) concentration. Inset: Nyquist plot for 50 mM potassium ferrocyanide in 50 mM HEPES, pH 7.4: AuNPs (black squares), AuNPs/RS + SDNA (blue squares), AuNPs/RS + SDNA + 0.1 nM complementary strand (CS) (grey squares). (For interpretation of the references to color in this figure legend, the reader is referred to the web version of this article.)

Considering the size of the nanoelectrodes and the volume sample, the ability of our system to achieve the detection of this concentration in a period of 30 min reconciles with the mass transport effects on biosensing at the nanoscale already addressed by Sheehan and Whitman, and Squires et al. [42,43].

4. Conclusions

In this work, we explored the effect on molecular recognition of different DNA immobilization strategies on 2 nm confined AuNP, a size scarcely studied as an independent transduction element in biosensors. Our results show that surface coverage and orientation of the immobilized strands play a key role in the sensitivity of the recognition process. A high strand coverage introduces a high background signal when the environment of the NPs is reduced to the molecular scale. Therefore, the co-immobilization of the single stranded DNA sequence with a short alkylthiol represents the most effective method for the modification of confined 2 nm AuNPs, in contrast to the methods chosen for the modification of planar surfaces [13] or free nanoparticles [17]. These results remark that the biomolecular recognition properties of the immobilized species in nanosized gold particles not only depend on its intrinsic affinity but also on its local environment.

Another important point is the selection of the EIS probe. Ferrocenemethanol, a neutral probe, has shown some changes indicating that the use of a molecular scale interface can be sensitive to the hindrance effect of structural changes; however, the charge repulsion introduced by a negative probe such as ferrocyanide is still a key factor in the electrochemical response.

This work shows that the adequate manipulation of a recognition element on a transductor at the nanoscale can produce a very sensitive device. The results observed as genosensor, achieving two order the magnitude less than the one observed as aptasensor, can be explained taking into account both the higher affinity of the strand for the complementary counterpart and the introduction of a higher number of negative charges, since the final occupied volume is practically the same [39,40]. Also, the use of impedance as detection method makes possible to work with samples of ion strength similar to real matrixes, in contrast to ionic conductance-based sensors that are only applicable in low salt concentration samples (typically 10 μM KCl) [44]. All these aspects can be considered as solid foundations for the development of miniaturized sensors.

Acknowledgments

This work was financially supported by the following grants: UBACYT 20020130100262BA (Universidad de Buenos Aires), XAFS2 beamline (LNLS, Brazil) proposal 17189, PICT-2011-0367, PIP-1035 (CONICET), OPCW and UNGS. MM., GAG., FGR, JMM and FB are CONICET members.

References

[1] J.C. Love, L.A. Estroff, J.K. Kriebel, R.G. Nuzzo, G.M. Whitesides, Self-assembled monolayers of thiolates on metals as a form of nanotechnology, Chem. Rev. 105 (2005) 1103–1170, https://doi.org/10.1021/cr0300789.
[2] K.M. Millan, A. Saraullo, S.R. Mikkelsen, Voltammetric DNA biosensor for cystic fibrosis based on a modified carbon paste electrode, Anal. Chem. 66 (1994) 2943–2948, https://doi.org/10.1021/ac00090a023.
[3] J. Wang, X. Cai, G. Rivas, H. Shiraishi, Stripping potentiometric transduction of DNA hybridization processes, Anal. Chim. Acta 326 (1996) 141–147, https://doi.org/10.1016/0003-2670(96)00042-6.
[4] F.R.R. Teles, L.P. Fonseca, Trends in DNA biosensors, Talanta 77 (2008) 606–623, https://doi.org/10.1016/j.talanta.2008.07.024.
[5] F. Li, J. Peng, Q. Zheng, X. Guo, H. Tang, S. Yao, Carbon nanotube-polyamidoamine dendrimer hybrid-modified electrodes for highly sensitive electrochemical detection of MicroRNA24, Anal. Chem. 87 (2015) 4806–4813, https://doi.org/10.1021/acs.analchem.5b00093.
[6] P. Abdul Rasheed, N. Sandhyarani, Quartz crystal microbalance genosensor for sequence specific detection of attomolar DNA targets, Anal. Chim. Acta 905 (2016) 134–139, https://doi.org/10.1016/j.aca.2015.11.033.

[7] E. Luzi, M. Minunni, S. Tombelli, M. Mascini, New trends in affinity sensing: aptamers for ligand binding, TrAC Trends Anal. Chem. 22 (2003) 810–818, https://doi.org/10.1016/S0165-9936(03)01208-1.
[8] Q. Guo, Y. Bao, X. Yang, K. Wang, Q. Wang, Y. Tan, Amplified electrochemical DNA sensor using peroxidase-like DNAzyme, Talanta 83 (2010) 500–504, https://doi.org/10.1016/j.talanta.2010.09.054.
[9] L. Cui, R. Peng, T. Fu, X. Zhang, C. Wu, H. Chen, H. Liang, C.J. Yang, W. Tan, Biostable L-DNAzyme for sensing of metal ions in biological systems, Anal. Chem. 88 (2016) 1850–1855, https://doi.org/10.1021/acs.analchem.5b04170.
[10] V.C. Ozalp, Acoustic quantification of ATP using a quartz crystal microbalance with dissipation, Analyst 136 (2011) 5046–5050, https://doi.org/10.1039/C1AN15762K.
[11] G. Papadakis, A. Tsortos, F. Bender, E.E. Ferapontova, E. Gizeli, Direct detection of DNA conformation in hybridization processes, Anal. Chem. 84 (2012) 1854–1861, https://doi.org/10.1021/ac202515p.
[12] H. Ceretti, B. Ponce, S.A. Ramírez, J.M. Montserrat, Adenosine reagentless electrochemical aptasensor using a phosphorothioate immobilization strategy, Electroanalysis 22 (2010) 147–150, https://doi.org/10.1002/elan.200900279.
[13] X. Zhang, V.K. Yadavalli, Surface immobilization of DNA aptamers for biosensing and protein interaction analysis, Biosens. Bioelectron. 26 (2011) 3142–3147, https://doi.org/10.1016/j.bios.2010.12.012.
[14] Z. Li, L. Zhang, H. Mo, Y. Peng, H. Zhang, Z. Xu, C. Zheng, Z. Lu, Size-fitting effect for hybridization of DNA/mercaptohexanol mixed monolayers on gold, Analyst 139 (2014) 3137–3145, https://doi.org/10.1039/C4AN00280F.
[15] A.S. Peinetti, H. Ceretti, M. Mizrahi, G.A. González, S.A. Ramírez, F.G. Requejo, J.M. Montserrat, F. Battaglini, Confined gold nanoparticles enhance the detection of small molecules in label-free impedance aptasensors, Nanoscale 7 (2015) 7763–7769, https://doi.org/10.1039/c5nr01429h.
[16] R. Campos, A. Kotlyar, E.E. Ferapontova, DNA-mediated electron transfer in DNA duplexes tethered to gold electrodes via phosphorothioated dA tags, Langmuir 30 (2014) 11853–11857, https://doi.org/10.1021/la502766g.
[17] W. Zhou, F. Wang, J. Ding, J. Liu, Tandem phosphorothioate modifications for DNA adsorption strength and polarity control on gold nanoparticles, ACS Appl. Mater. Interfaces 6 (2014) 14795–14800, https://doi.org/10.1021/am504791b.
[18] J.-S. Lee, D.S. Seferos, D.A. Giljohann, C.A. Mirkin, Thermodynamically controlled separation of polyvalent 2-nm gold nanoparticle-oligonucleotide conjugates, J. Am. Chem. Soc. 130 (2008) 5430–5431, https://doi.org/10.1021/ja800797h.
[19] E. Gonzalez Solveyra, I. Szleifer, What is the role of curvature on the properties of nanomaterials for biomedical applications? Wiley Interdiscip. Rev. Nanomed. Nanobiotechnol. 8 (2016) 334–354, https://doi.org/10.1002/wnan.1365.
[20] A.S. Peinetti, S. Herrera, G.A. Gonzalez, F. Battaglini, Synthesis of atomic metal clusters on nanoporous alumina, Chem. Commun. 49 (2013) 11317–11319, https://doi.org/10.1039/C3CC47170E.
[21] D.E. Huizenga, J.W. Szostak, A DNA aptamer that binds adenosine and ATP, Biochemistry 34 (1995) 656–665, https://doi.org/10.1021/bi00002a033.
[22] A. Ulman, Formation and structure of self-assembled monolayers, Chem. Rev. 96 (1996) 1533–1554, https://doi.org/10.1021/cr9502357.
[23] B. Ravel, M. Newville, ATHENA, ARTEMIS, HEPHAESTUS: data analysis for X-ray absorption spectroscopy using IFEFFIT, J. Synchrotron Radiat. 12 (2005) 537–541, https://doi.org/10.1107/S0909049505012719.
[24] Z. Li, R. Jin, C.A. Mirkin, R.L. Letsinger, Multiple thiol-anchor capped DNA–gold nanoparticle conjugates, Nucleic Acids Res. 30 (2002) 1558–1562.
[25] J.M. Ramallo-López, L.J. Giovanetti, F.G. Requejo, S.R. Isaacs, Y.S. Shon, M. Salmeron, Molecular conformation changes in alkylthiol ligands as a function of size in gold nanoparticles: X-ray absorption studies, Phys. Rev. B 74 (2006), 73410. .
[26] D.J. Lewis, T.M. Day, J.V. MacPherson, Z. Pikramenou, Luminescent nanobeads: attachment of surface reactive Eu(iii) complexes to gold nanoparticles, Chem. Commun. 0 (2006) 1433, https://doi.org/10.1039/b518091k.
[27] L. Strong, G.M. Whitesides, Structures of self-assembled monolayer films of organosulfur compounds adsorbed on gold single crystals: electron diffraction studies, Langmuir 4 (1988) 546–558, https://doi.org/10.1021/la00081a009.
[28] E. Katz, I. Willner, Probing biomolecular interactions at conductive and semiconductive surfaces by impedance spectroscopy: routes to impedimetric immunosensors, DNA-sensors, and enzyme biosensors, Electroanalysis 15 (2003) 913–947, https://doi.org/10.1002/elan.200390114.
[29] K. Zen, C.-Y. Zhang, Circulating MicroRNAs: a novel class of biomarkers to diagnose and monitor human cancers, Med. Res. Rev. 32 (2012) 326–348, https://doi.org/10.1002/med.20215.
[30] T. Hermann, D.J. Patel, Adaptive recognition by nucleic acid aptamers, Science 287 (2000) 820–825http://science.sciencemag.org/content/287/5454/820.abstract.
[31] R. Owczarzy, B.G. Moreira, Y. You, M.A. Behlke, J.A. Walder, Predicting stability of DNA duplexes in solutions containing magnesium and monovalent cations, Biochemistry 47 (2008) 5336–5353, https://doi.org/10.1021/bi702363u.
[32] J. SantaLucia, D. Hicks, The thermodynamics of DNA structural motifs, Annu. Rev. Biophys. Biomol. Struct. 33 (2004) 415–440, https://doi.org/10.1146/annurev.biophys.32.110601.141800.
[33] M.C. Rodriguez, A.-N. Kawde, J. Wang, Aptamer biosensor for label-free impedance spectroscopy detection of proteins based on recognition-induced switching of the surface charge, Chem. Commun. (2005) 4267–4269, https://doi.org/10.1039/B506571B.
[34] A.S. Peinetti, R.S. Gilardoni, M. Mizrahi, F.G. Requejo, G.A. González, F. Battaglini, Numerical simulation of the diffusion processes in nanoelectrode arrays using an axial neighbor symmetry approximation, Anal. Chem. 88 (2016) 5752–5759, https://doi.org/10.1021/acs.analchem.6b00039.
[35] M. Fleischmann, S. Pons, The behavior of microdisk and microring electrodes. Mass transport to the disk in the unsteady state: The ac response, J. Electroanal. Chem. Interfacial Electrochem. 250 (1988) 277–283, https://doi.org/10.1016/0022-0728(88)85169-6.
[36] R. Ferrigno, H.H. Girault, Finite element simulation of electrochemical ac diffusional impedance. Application to recessed microdiscs, J. Electroanal. Chem. 492 (2000) 1–6, https://doi.org/10.1016/S0022-0728(00)00236-9.
[37] S.M. Rezaei Niya, M. Hoorfar, On a possible physical origin of the constant phase element, Electrochim. Acta 188 (2016) 98–102, https://doi.org/10.1016/j.electacta.2015.11.142.
[38] H.-K. Song, H.-Y. Hwang, K.-H. Lee, L.H. Dao, The effect of pore size distribution on the frequency dispersion of porous electrodes, Electrochim. Acta 45 (2000) 2241–2257, https://doi.org/10.1016/S0013-4686(99)00436-3.
[39] C.H. Lin, D.J. Patel, Structural basis of DNA folding and recognition in an AMP-DNA aptamer complex: distinct architectures but common recognition motifs for DNA and RNA aptamers complexed to AMP, Chem. Biol. 4 (1997) 817–832.
[40] J.M. Berg, J.L. Tymoczko, G.J. Gatto, L. Stryer, Biochemistry, 8th ed. W.H. Freeman, New York, 2015.
[41] L. Jiang, H. Zhang, J. Zhuang, B. Yang, W. Yang, T. Li, C. Sun, Sterically mediated two-dimensional architectures in aggregates of au nanoparticles directed by phosphorothioate oligonucleotide-DNA, Adv. Mater. 17 (2005) 2066–2070, https://doi.org/10.1002/adma.200402004.
[42] P.E. Sheehan, L.J. Whitman, Detection limits for nanoscale biosensors, Nano Lett. 5 (2005) 803–807, https://doi.org/10.1021/nl050298x.
[43] T.M. Squires, R.J. Messinger, S.R. Manalis, Making it stick: convection, reaction and diffusion in surface-based biosensors, Nat. Biotechnol. 26 (2008) 417–426, https://doi.org/10.1038/nbt1388.
[44] X. Wang, S. Smirnov, Label-free DNA sensor based on surface charge modulated ionic conductance, ACS Nano 3 (2009) 1004–1010, https://doi.org/10.1021/nn900113x.